OPTIMIZING THE PARAMETERS OF CELL EXPANSION IN ALKALINE MANGANESE DIOXIDE BUTTON CELLS

K. TAKEDA

Seiko Electronic Components Ltd., 563 Takatsukashinden, Matsudo-shi, Chiba 271 (Japan)

(Received October 3, 1989)

Summary

The optimization of the parameters of cell expansion during discharge in alkaline manganese dioxide button cells is studied. The cell expansion after discharge and overdischarge is reduced by optimizing technological parameters, such as the type of MnO_2, the amount and the size of graphite, the pressure for cathode pellets, and the amount of electrolyte in anode and cathode mixes. Other parameters, like the amount of anode and cathode mixes, concentration of electrolyte, the amount of binder in the cathode mix, the types of absorbent and separator are independent of the cell expansion. From studies of the morphology of the cathode mix after discharge, vacancy and agglomeration appeared in a more significant level than the cathode mix before discharge.

Introduction

In alkaline manganese dioxide button cells, cell expansion occurs during discharge and overdischarge due to swelling of the MnO_2 cathode. The cell expansion greatly affects small electronic instruments such as watches and calculators. The expansion of MnO_2 during discharge has been reported by Kozawa [1]. There is scope, however, for further research. In order to reduce cell expansion, a study has been made here of the optimization of parameters of cell expansion from the viewpoints of design of the cell and cathode as well as the technology of alkaline manganese dioxide button cells.

Experimental

All experiments were carried out using standard Zn/MnO_2 cells (LR44). Figure 1 shows the structure of an LR44 alkaline manganese dioxide button cell. The design uses a can stamped from a nickel-plated steel sheet or a steel sheet that is electroplated on both sides with a thin layer of nickel. The can

0378-7753/90/$3.50

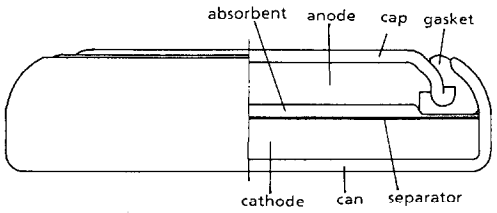

Fig. 1. Structure of LR44 alkaline MnO_2 button cell.

serves as the positive pole of the cell. The cap, made from chromium–nickel sheet and electroplated on one side with a thin layer of copper, serves as the negative pole.

The cathode of the cell is a mixture of manganese dioxide, graphite and binder. This is pressed to a pellet and placed in the can. The anode is a mixture of amalgamated zinc powder and electrolyte. Sodium carboxymethyl cellulose serves as a gelling agent. The anode material is injected into the cap. The cathode is isolated from the anode by absorbent and separator. The absorbent is composed of non-woven pulp or paper while the separator consists of kraft paper or cellophane. The electrolyte is an aqueous solution of potassium hydroxide.

The ring gasket is made from a special type of polyamide by injection molding. The gasket is subjected to an additional treatment in order to increase its mechanical strength. Also, in order to prolong its storage life and operational life, the gasket is hermetically sealed by locating it between the can and the cap. Hermetically-sealed batteries feature a high capacity and also operate over a wide range of current drains.

Figure 2 shows the cause and effect diagram for the cell expansion after discharge. The cell was assembled by using an L_{16} orthogonal array experimental design method. The most probable factors, selected out of many, are shown in Fig. 2. The cell expansion (ΔH) is defined as:

$$\Delta H = H_1 - H_0 \tag{1}$$

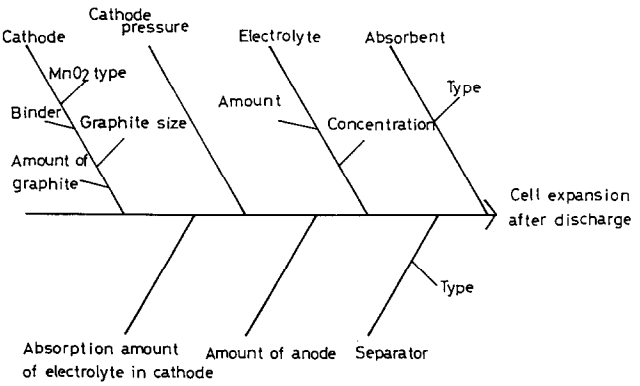

Fig. 2. Cause and effect diagram.

where H_0 = height of cell before discharge and H_1 = height of cell after discharge.
The discharge was continuously carried out at loads of 100 Ω, 1.5 kΩ and 3 kΩ to a cut-off voltage of 1.2 V, and at normal temperature.

Results and discussion

Table 1 shows the analysis of variance by using the experimental design method (L_{16}). The symbols *, ** and Δ are the ranking in significance. Symbol P is the contribution ratio. Classification of experimental conditions is represented by the symbols I, II, III, IV. The unit used in the data is the expansion of the cell per capacity at R_L = 1.5 kΩ, and cut-off voltage of 1.2 V, *i.e.*, μm/mA h.

As shown in Table 1, the most influential factors are the type of MnO_2, the pressure for cathode pellets, and the amount of electrolyte in the anode

TABLE 1
Analysis of variance (unit = μm/mA h)

Factor	Level significance	P (%)	Experimental conditions			
			I	II	III	IV
1 MnO_2 type	**	6.5	A 1.38	B 1.42	C 1.51	D 1.16
2 Amount of graphite (%)	*	4.1	2.5 1.51	5 1.20	7.5 1.21	10 1.44
3 Graphite size (μm)	Δ	5.3	2.5 1.27	5 1.46		
4 Binder (%)			0 1.33	3 1.40		
5 Cathode pressure (ton)	Δ	6.8	4 1.26	6 1.47		
6 Electrolyte in cathode (μl)	Δ	5.5	50 1.46	60 1.27		
7 Amount of anode (mg)			180 1.40	160 1.33		
8 Amount of electrolyte (μl)	*	8.1	80 1.48	90 1.25		
9 Concentration of electrolyte (%)			35 1.31	40 1.43		
10 Absorbent type			A 1.36	B 1.37		
11 Separator type			A 1.31	B 1.42		

mix. The next influential factors are the amount and the size of the graphite, and the amount of electrolyte in the cathode mix. The effect of the amount of binder in the cathode mix, the amount of the anode mix, the concentration of the electrolyte, and the type of absorbent and separator, is negligible. Moreover, the cell expansion increases with regard to the discharge rate and the capacity. The cell expansion stops, however, within the limit. In further tests, the cell expansion was found to be independent of the amount of the cathode mix and the value of the discharge resistance. In detail, the influence of the various parameters is as follows.

Type of MnO_2

Figure 3 shows the influence of different types of MnO_2 in terms of the density of the cathode pellet, the discharge capacity of the cell, and the cell expansion. MnO_2 type D is minimum in relation to the cell expansion and MnO_2 type A is maximum in relation to the discharge capacity. Table 2 shows a typical analysis of the electrolytic MnO_2 used in Fig. 3. It can be seen that MnO_2 type D has the finest particles and the smallest apparent density.

Amount of graphite

Figure 4 shows the influence of different amounts of graphite on the cathode density of the pellet, the discharge capacity of the cell and the cell expansion. The results indicate that the cathode density is greatest and the cell expansion smallest when the amount of graphite is 5 wt.%.

Size of graphite

As shown in Table 1, the cell expansion decreases with decrease in the graphite size from 5 μm to 2.5 μm.

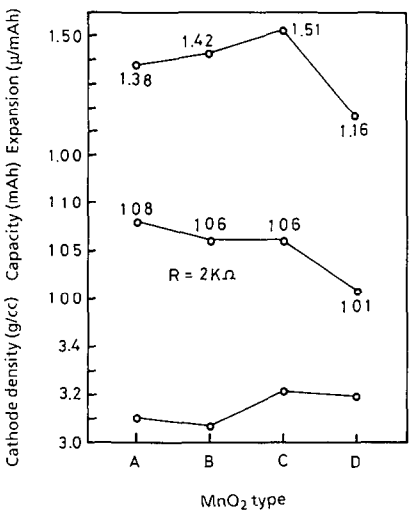

Fig. 3. Dependence of cell characteristics on type of MnO_2.

TABLE 2

Typical analysis of electrolytic MnO_2

	MnO_2 type			
	A	B	C	D
Chemical analysis				
MnO_2 (%)	92.0	92.0	92.2	92.2
Total Mn (%)	60.0	60.0	60.2	60.2
Physical properties				
Moisture (%)	1.46	1.49	1.50	1.50
Particle size (%)	7.6	7.6	10.0	0.1
+200 mesh (74 μm)				
−200 mesh (74 μm)	92.4	92.4	90.0	99.9
−325 mesh (44 μm)	73.1	73.1	60.0	93.0
Apparent density JIS method (g cm^{-3})	1.77	1.77	1.61	1.49
Electrochemical properties				
pH (D. water method)	5.5	6.4	8.3	8.3

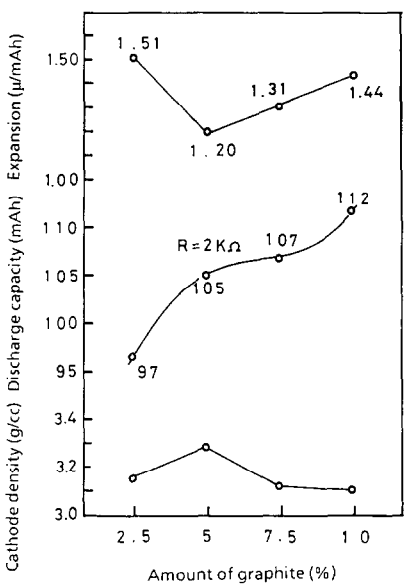

Fig. 4. Dependence of cell characteristics on amount of graphite.

Amount of binder

No substantial difference in the cell expansion is observed for 0 wt.% and 3 wt.% of binder in the cathode mix (Table 1).

Pressure of pellet

As observed in Table 1, the cell expansion at 4 ton is smaller than that at 6 ton (diameter of the pellet = 10.5 mm). Figure 5 presents the discharge curve and the cell expansion as a function of pellet pressure. The data clearly demonstrate that the cell expansion after discharge and overdischarge is reduced at lower pressures.

Amount of electrolyte in cathode mix

The cell expansion is smaller when the amount of electrolyte in the cathode mix is reduced from 60 μl to 50 μl (Table 1).

Amount of anode

No substantial difference in the cell expansion is observed at 160 mg (theoretical = 117 mA h) and 180 mg (theoretical = 131 mA h) of anode (Table 1).

Amount of electrolyte in anode mix

The cell expansion is smaller when the amount of electrolyte in the anode mix is reduced from 90 μl to 80 μl (Table 1).

Electrolyte concentration

Figure 6 shows the discharge curve and cell expansion in terms of KOH concentration; the cell was discharged under a load of 100 Ω and at normal temperature. The discharge capacity is small for 25% and 30% KOH. No significant difference in the cell expansion is observed with 35%, 38% and 40% KOH.

Type of absorbent

As shown in Table 1, no substantial difference in the cell expansion is observed between non-woven paper made from a mixture of vinylon and rayon, and paper composed of mercerized kraft pulp.

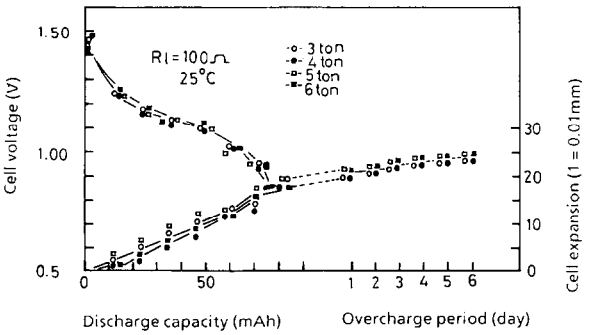

Fig. 5. Discharge curve and cell expansion as a function of pellet pressure.

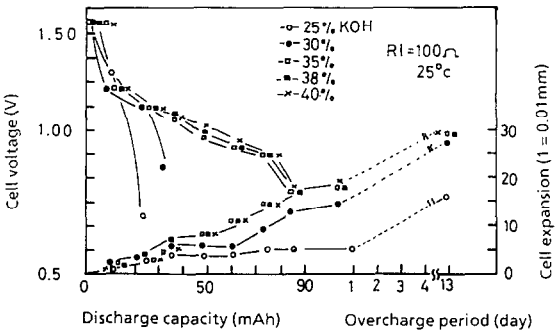

Fig. 6. Discharge curve and cell expansion in terms of KOH concentration.

Type of separator

No significant difference in the cell expansion is observed between kraft paper and cellophane (Table 1).

Amount of cathode mix

Figure 7 gives the discharge curve and the cell expansion in terms of the amount of the cathode mix. The theoretical capacity of the cathode mix is 115 mA h and 163 mA h for 450 mg and 640 mg of cathode mix, respectively. The theoretical capacity of the anode is 131 mA h. The cell was discharged under a load of 3 kΩ at normal temperature.

When discharging to a cut-off voltage of 1.2 V, the cell expansion increases as the amount of cathode mix increases, *i.e.*, the discharge capacity is 104 mA h (640 mg) and 83 mA h (450 mg). The cell expansion increases at a cut-off voltage of 0.9 V and stops within the limit. The cell expansion per discharge capacity to a cut-off voltage of 1.2 V is 1.6 μm/mA h (640 mg) and 1.5 μm/mA h (450 mg).

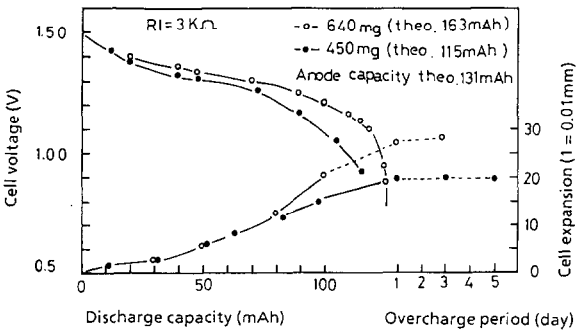

Fig. 7. Discharge curve and cell expansion in terms of amount of cathode mix.

Discharge load

Figure 8 presents the dependence of cell expansion on discharge capacity under various discharge loads. No substantial difference in the cell expansion is observed at 100 Ω, 1.5 kΩ and 3 kΩ.

Morphology of cathode mix before and after discharge

Figure 9 shows the sectional view of the alkaline cell (LR44) before and after discharge obtained by using a scanning electron microscope (SEM). The

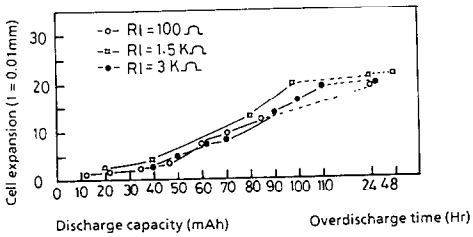

Fig. 8. Cell expansion *vs.* discharge capacity for various discharge loads.

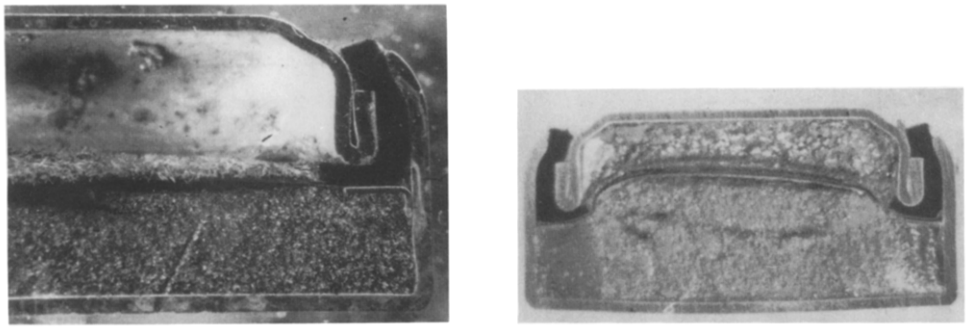

(a) (b)

Fig. 9. Alkaline cell (LR44): (a) before discharge; (b) after discharge.

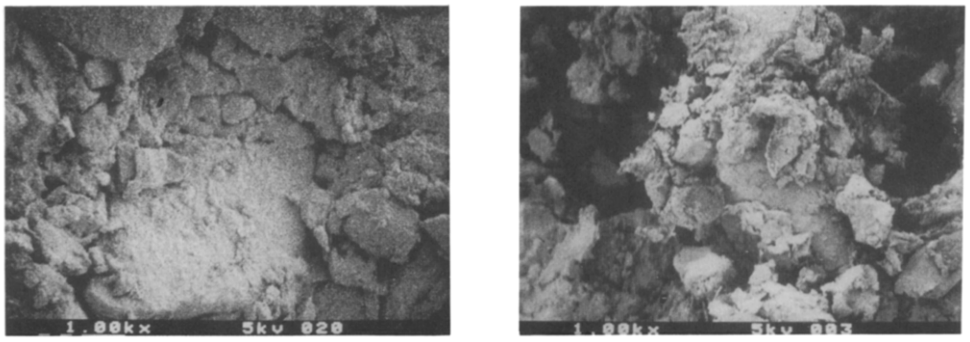

(a) (b)

Fig. 10. Surface of cathode mix for alkaline cell (LR44): (a) before discharge; (b) after discharge (1000× magnification).

micrographs reveal that the cathode expands to a great extent after discharge. Electron micrographs of the surface of the cathode mix before and after discharge are given in Fig. 10. The battery was discharged to a cut-off voltage of 1.2 V under a load of 2 kΩ, and at room temperature. A remarkable morphological change in the cathode mix is observed. In particular, the material agglomerates and becomes more porous (Fig. 10(b)).

Conclusions

The cell expansion after discharge and overdischarge is reduced by optimizing technological parameters such as the type of MnO_2, the amount and size of graphite, the pressure of the cathode pellets, and the amount of electrolyte in the anode and cathode mixes.

Acknowledgements

The author is grateful to T. Fukuchi (Seiko Instruments Inc.) for conducting the experimental investigations and also to Seiko Electronic Components Ltd. for permission to publish the findings. The author acknowledges the analytical support by Seiko I Techno Research Co., Ltd.

Reference

1 A. Kozawa, *Denki Kagaku*, *47* (1979) 642.